

Incommensurate antiferromagnetism in FeAl₂: Magnetic, Mössbauer, and neutron diffraction measurements

D. Kaptás,^{1,*} E. Sváb,¹ Z. Somogyvári,¹ G. André,² L. F. Kiss,¹ J. Balogh,¹ L. Bujdosó,¹ T. Kemény,¹ and I. Vincze¹

¹Research Institute for Solid State Physics and Optics, H-1525 Budapest P.O. Box 49, Hungary

²Laboratoire Leon Brillouin (CEA-CNRS), CEA/Saclay, 91191 Gif-sur-Yvette, France

(Received 14 September 2005; published 9 January 2006)

Magnetic, Mössbauer, and neutron diffraction measurements were used to study the anomalous magnetic behavior of FeAl₂. The magnetization is almost linear with the applied field up to 14 T at 5 K. The Fe-Al system Mössbauer measurement in the 7 T external magnetic field clearly shows the presence of canted, antiferromagnetically coupled Fe magnetic moments. Neutron diffraction indicates an incommensurate magnetic structure with a periodicity of about 1.1 nm.

DOI: [10.1103/PhysRevB.73.012401](https://doi.org/10.1103/PhysRevB.73.012401)

PACS number(s): 75.25.+z, 75.50.Ee, 76.80.+y, 74.25.Ha

The research of the magnetic properties of bcc Fe-Al alloys has been since long in the center of interest because of the simple atomic structure and the complicated, spin-glass-like magnetic behavior following ferromagnetism above 30 at. % Al content.¹ Based on an early hypothesis,² it is often believed that antiparallel Fe magnetic moments of the antiferromagnetic Fe-Al-Fe superexchange may explain the magnetic anomalies. However, no unambiguous evidence was found for the existence of oppositely oriented magnetic moments. Recent neutron diffraction investigation³ reveals incommensurate spin density waves with spins closely parallel on the nearest Fe neighbors. The Al-rich Fe-Al alloys were thought to be nonmagnetic just like the well-ordered bcc FeAl. With this background, the report of spin-glass behavior in FeAl₂ deduced from susceptibility⁴ and Mössbauer⁵ measurements was surprising. In the following it will be shown that the magnetic structure is incommensurate and direct evidence will be presented for the existence of antiferromagnetically coupled Fe magnetic moments in this alloy via external magnetic field dependent ⁵⁷Fe Mössbauer study.

The stoichiometric FeAl₂ ingot was prepared from the pure components by induction melting in a cold crucible and annealing at 850 °C for four days similar to Ref. 4. The sample was examined by x-ray and neutron diffraction, magnetization measurements, and Mössbauer spectroscopy. The neutron diffraction measurements were carried out on the G4.1 diffractometer in LLB, Saclay.⁶ Data were collected at six temperatures from 1.5 K up to 45 K with 2.4266 Å wavelength neutrons in the 4°–84° 2θ scattering angle region. A Quantum Design MPMS-5S SQUID (superconducting quantum interference device) magnetometer with a maximum field of 5 T was used for the magnetisation measurements. ⁵⁷Fe Mössbauer spectra were recorded by a standard constant acceleration spectrometer using a 50 mCi ⁵⁷CoRh source at room temperature. The measurements were performed with and without external magnetic fields between 4.2 and 300 K. The magnetic field was applied parallel to the γ-beam using a 7 T Janis superconducting magnet. The isomer shift data are given with respect to α-Fe at room temperature. The spectra were evaluated in a standard manner, at low temperatures the magnetic component was analyzed by binomial distributions.⁷

The simultaneous Rietveld analysis of the room temperature x-ray and neutron diffraction patterns gave similar results to those reported⁷ for a triclinic unit cell: $a=0.4875$, $b=0.6462$, and $c=0.8787$ nm; $\alpha=91.88^\circ$, $\beta=73.29^\circ$, and $\gamma=96.90^\circ$ were found. The obtained atomic positions and occupations are slightly different from those reported in Ref. 8, but obviously the character of the structure and the neighbor relations remained unchanged. Although the structure of Corby and Black⁸ well describes the neutron and x-ray spectra, apparent systematical deviations in the intensity of some reflections and the presence of a low-intensity extra reflections were found. The x-ray, neutron diffraction and Mössbauer measurements excluded a detectable trace of any impurity phase (FeAl, Fe₃Al, Fe₄Al₁₃, Fe₂Al₅, FeAl₆, Al₂O₃).

The structure of Ref. 8, can be described as an irregular closed-packed arrangement of Fe and Al atoms. The stoichiometric unit cell has 18 atoms: 12 Al and 6 Fe. The Fe atoms are surrounded by three to five nearest Fe neighbors. It is difficult to reconcile this structure with the room temperature Mössbauer spectrum of Fig. 1. It clearly shows the presence of two different iron environments, designated as Fe_h and Fe_l, with no detectable amount of disorder (i.e., no line broadening is observed). The relative occupation of the two sites was found to be Fe_h:Fe_l=1:2. The two sites have about the same quadrupole splitting: 0.432(2) and 0.451(1) mm/s,

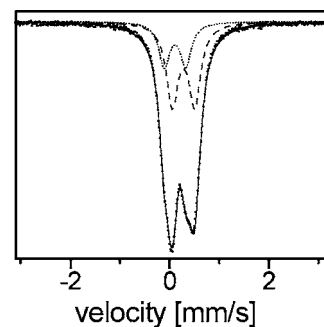


FIG. 1. Room temperature Mössbauer spectrum of FeAl₂. Full line is the fitted curve consisting of two quadrupole doublets, the Fe_h and the Fe_l components are marked by the dotted and broken lines, respectively.

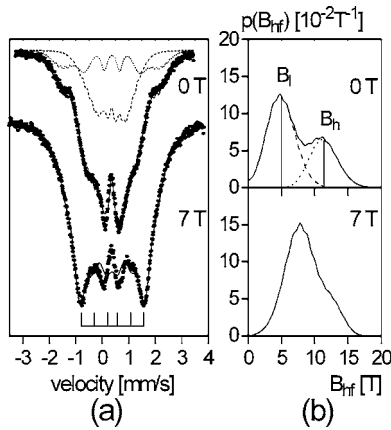


FIG. 2. Mössbauer spectra of FeAl_2 at 4.2 K (a) and the respective Fe hyperfine field distributions (b) in 7 T and without applied magnetic field; full lines are the fitted curves. The components of the Fe_h and Fe_l environments are shown as the dotted and broken lines, respectively. For 7 T the comb shows the positions of the six-line pattern of the average hyperfine field.

but significantly different isomer shifts: $\text{IS}(\text{Fe}_h) = 0.108(2)$ mm/s and $\text{IS}(\text{Fe}_l) = 0.278(1)$ mm/s, respectively. The isomer shift values are characteristic to the nearest neighbor environments in the Fe-Al system: larger values correspond to more Al first neighbors according to the data of ordered bcc alloys. Fe_3Al has DO_3 structure with two kind of Fe environments. FeI has four Fe and four Al, FeII has eight Fe first neighbors, and the isomer shifts are $\text{IS}(\text{FeI}) = 0.19$ mm/s and $\text{IS}(\text{FeII}) = 0.07$ mm/s, respectively. FeAl has a B2 structure, all Fe atoms are surrounded by 8 Al nearest neighbors, the isomer shift is 0.26 mm/s. Although the values of the isomer shifts are also influenced by the nearest neighbor distances, if we assume a close packed structure our data suggest that the Fe_h atoms have 6 ± 1 Fe and the Fe_l atoms have 3 ± 1 Fe nearest neighbors. These values were deduced by assuming that due to the stoichiometry Fe atoms have on average four Fe nearest neighbors out of the supposed 12 of a close packed structure.

The Mössbauer spectrum measured at 4.2 K is shown in Fig. 2(a). The lines are structureless and quite broad, individual hyperfine patterns cannot be resolved, but the hyperfine field distribution shown in Fig. 2(b) can be determined. However, our spectra measured both at room and liquid helium temperature show more structure than those of Ref. 5, which suggests a larger disorder in that sample. Two peaks can be distinguished in the hyperfine distribution as shown in the figure, the ratio of the respective areas under the subdistributions is 2:1, the same as determined for the quadrupole doublets of the room temperature paramagnetic spectrum. Accordingly, the two peaks around B_l and B_h are attributed to the Fe_l and Fe_h sites. The isomer shifts of these magnetic components support this assignment: the sites denoted by Fe_h have lower values as it is obvious from the spectrum of Fig. 2(a). The average values of these subcomponents are $B_h = 11.3$ T and $B_l = 4.8$ T, respectively. These are related to the values of the individual Fe magnetic moments. It is well known,⁹ that in Fe-based dilute alloys more than 50% of the Fe hyperfine field originates from the conduction electron

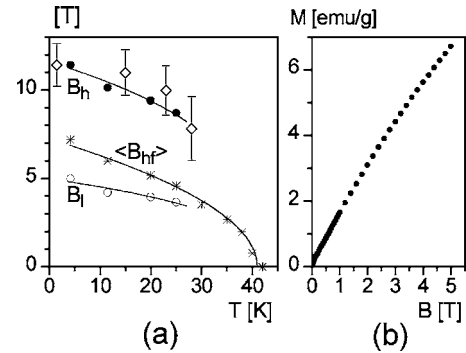


FIG. 3. Temperature dependence of the average Fe hyperfine field, $\langle B_{hf} \rangle$ (stars), the B_h (dots), and the B_l (circles) components in FeAl_2 (a) and the applied magnetic field dependence of the magnetization measured at 5 K (b). The empty rhombs are the square root of the area of the stronger peak (12.9°) normalized to B_h at low temperature. The lines are guides to the eye.

contribution of the magnetic neighbors. Similar relation remains valid¹⁰ in the bcc Fe-Al alloys around Fe_3Al . On the other hand, in close packed intermetallic compounds the neighbor contribution is less than 10% and the Fe hyperfine field is in a good approximation proportional to the Fe magnetic moment with a proportionality constant of $13 \text{ T}/\mu_B$.¹¹ This assumption would give about $0.9\mu_B$ and $0.4\mu_B$ for the iron magnetic moments in the Fe-rich and Fe-poor environments, respectively. The standard width of the hyperfine field distribution around the B_h component is about 2 T, a somewhat large value if it were attributed to dipole contributions solely. The anisotropy of the local spin polarization found¹² in complex magnetic spin structures may explain this value.

Figure 3(a) shows the average of the hyperfine field distribution, $\langle B_{hf} \rangle$, B_h , and B_l as a function of the temperature. Within the error of the evaluation B_h and B_l follow the same reduced curve, this behavior is characteristic of metallic and intermetallic alloys. At higher temperatures the determination of B_h and B_l is problematic, only $\langle B_{hf} \rangle$ is shown. No magnetic broadening of the quadrupole doublet is observed at and above 42 K, thus a magnetic transition temperature $T_i = 41$ K is deduced.

Diffraction patterns measured at 34 K and 45 K could be well described by pure nuclear scattering. Between 1.5 K and 28 K the presence of two additional magnetic peaks were observed at 12.97° and 17.2° scattering angles, indicated by arrows in the inset of Fig. 4. The position and the area of these peaks are temperature dependent. As the peaks are rather narrow, though slightly broadened compared to the nuclear reflections, a long-range ordering of the magnetic moments can be stated. This behavior is in contradiction with the reported^{4,5} spin-glass type of arrangement of the moments. The first magnetic peak is shifted toward higher scattering angles, while the second one shifted toward smaller angles with increasing temperature, indicating their satellite reflection character, the shift is 0.25° for both magnetic peaks in the investigated temperature range. At the same time, the position of the nuclear reflections does not change (except a negligible shift due to thermal expansion), and the magnetic ordering does not give a scattering contribution to these

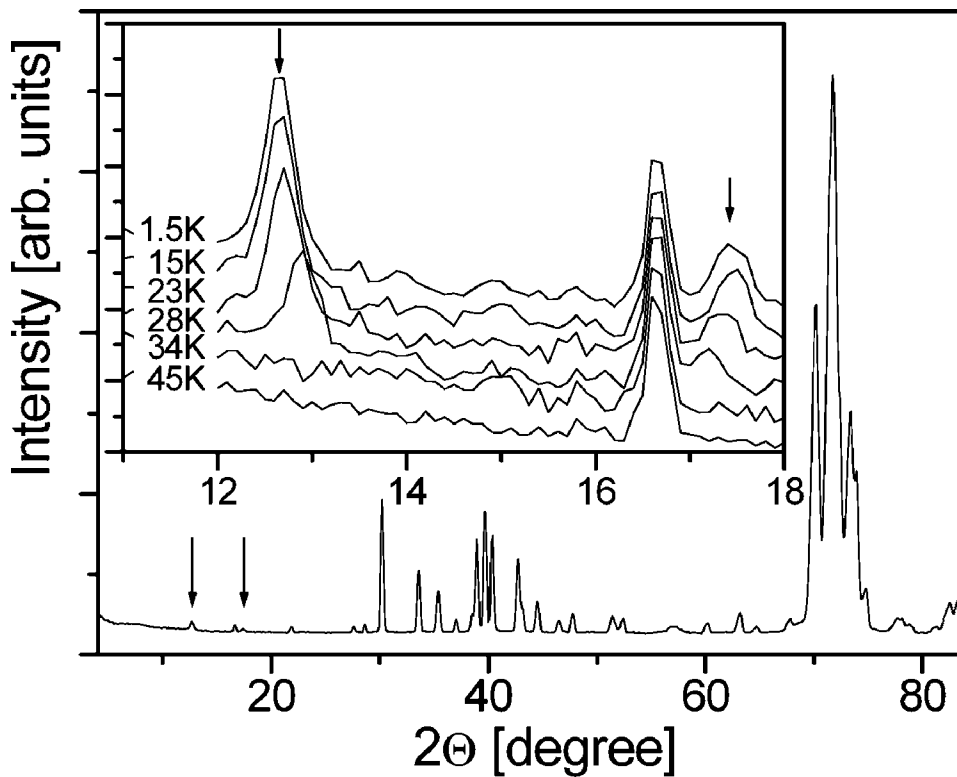


FIG. 4. Neutron diffraction pattern of FeAl_2 at 1.5 K ($\lambda = 2.4266 \text{ \AA}$). The inset shows the low angle part taken at different temperatures between 1.5–45 K. Arrows indicate the temperature-dependent weak magnetic satellite reflections, showing the formation of long-range ordered incommensurate magnetic structure.

peaks. From this observation the incommensurate nature of the magnetic structure can be concluded. The incommensurate period of the magnetic structure can be determined, assuming that the reflection at $\sim 12.9^\circ$ can be indexed as $\pm \mathbf{k}$, where \mathbf{k} is the magnetic propagation vector. Thus we get a period length of 1.1 nm. Unfortunately, the diffraction pattern does not contain enough information to precisely determine the direction of the \mathbf{k} vector. After trying several possible directions, $\mathbf{k} \parallel (1\ 0\ 0)$ seems to be promising, as in this case the position of the $(1\ 0\ 0) - \mathbf{k}$ satellite coincides with the magnetic peak at 17.2° . The observed magnetic peaks have very low intensities, indicating small ordered magnetic moments. The two peaks of magnetic origin are not sufficient for the determination of the magnetic structure, thus the exact quantitative analysis of the magnetic moments is not possible from the present neutron diffraction data, they are in the range of $0.3\text{--}0.5 \mu_B$. The square root of the area of the stronger peak (12.9°) normalized to B_h at low temperature is shown in Fig. 3(a) as a function of the temperature. This quantity is roughly proportional to the magnetic moment and the agreement with the Mössbauer data is acceptable. According to the neutron measurements the magnetic transition temperature should be somewhat less than 34 K (Fig. 4), at least the long range order disappears at this temperature, but the existence of a short range order above this temperature may explain the somewhat larger T_i found in the Mössbauer measurement. It should be noted that no sign of superparamagnetic behavior characteristic of magnetic clusters was found in our Mössbauer measurements at 100 K in 7 T external magnetic field.

The magnetization measured at 5 K up to 5 T is shown in Fig. 3(b). It is almost linear as a function of the applied field and this behavior remains valid¹³ up to 14 T, which means a

nearly complete compensation of the magnetic moments.

Information from Mössbauer spectroscopy on the direction of the Fe magnetic moments is given by the relative intensity of the second and fifth lines, $I_{2,5}$ of the magnetically split spectra (corresponding to the $\Delta m = 0$ nuclear transitions). $I_{2,5} = 4 \sin^2 \theta / (1 + \cos^2 \theta)$, where θ is the angle between the magnetic moment and the magnetic field B_{ext} applied parallel to the γ -beam direction. $I_{2,5} = 2$ corresponds to a random Fe spin orientation and this value was found without the applied field. For complete saturation, i.e., in the case when all magnetic moments are collinear to B_{ext} , $I_{2,5} = 0$.

The hyperfine field is oriented antiparallel to the magnetic moment. In collinear ferromagnetic state the absolute value of the hyperfine field should decrease with the value of the applied field, in the case of canting the decrease is $B_{ext} \cos \theta$. Obviously, the hyperfine field of antiferromagnetically coupled magnetic moments should increase with this amount. The Mössbauer spectrum measured at 4.2 K in $B_{ext} = 7$ T external magnetic field is shown in Fig. 2. The shape of the spectra are considerably different in $B_{ext} = 0$ and 7 T and it is clear that the second and fifth lines do not disappear (i.e., $I_{2,5} \neq 0$) and a small increase (about 1.3 T) of the average hyperfine field is observed. The shape of the hyperfine field distribution and the value of $I_{2,5}$ is strongly correlated, thus the hyperfine field distribution shown in 7 T [Fig. 2(b)] has a large uncertainty because of systematical errors. The most significant difference with respect to the 0 T distribution is the increase of the hyperfine field of the low field part of the distribution and some decrease in the intensity of the second and fifth lines of the spectra. It is well seen in the measured spectrum at 7 T: the relative absorption in the low velocity range decreases and the high velocity shoulders disappear. The components with increased hyperfine

field are infallible fingerprints of antiferromagnetically oriented Fe magnetic moments. It is possible to give a rough estimate of the magnetic field where complete saturation would be reached, i.e., where the observed incommensurable antiferromagnetic structure would be ferromagnetic. The magnetization at 5 K in 5 T [Fig. 3(b)] gives an average Fe magnetic moment of $\approx 0.13\mu_B$ and the saturation value estimated on the base of the Mössbauer hyperfine fields is $\approx 0.54\mu_B$. The comparison of these values gives 22–25 T for

the strength of the magnetic field necessary to align the magnetic moments. It obviously cannot be explained with usual magnetic anisotropy values.

ACKNOWLEDGMENTS

This work was supported by the Hungarian Research Fund (OTKA T 31854 and T42495).

*Electronic address: kaptas@szfki.hu

- ¹R. D. Shull, H. Okamoto, and P. A. Beck, *Solid State Commun.* **20**, 863 (1976); W. Bao, S. Raymond, S. M. Shapiro, K. Motoya, B. Fåk, and R. W. Erwin, *Phys. Rev. Lett.* **82**, 4711 (1999).
²H. Sato and A. Arrott, *Phys. Rev.* **114**, 1427 (1959).
³D. R. Noakes, A. S. Arrott, M. G. Belk, S. C. Deevi, Q. Z. Huang, J. W. Lynn, R. D. Shull, and D. Wu, *Phys. Rev. Lett.* **91**, 217201 (2003); D. R. Noakes, A. S. Arrott, M. G. Belk, S. C. Deevi, J. W. Lynn, R. D. Shull, and D. Wu, *J. Appl. Phys.* **95**, 6574 (2004).
⁴C. S. Lue, Y. Öner, D. G. Naugle, and J. H. Ross, Jr., *Phys. Rev. B* **63**, 184405 (2001).
⁵J. Chi, Y. Li, F. G. Vagizov, V. Goruganti, and J. H. Ross, Jr.,

Phys. Rev. B **71**, 024431 (2005).

- ⁶<http://www-llb.cea.fr/spectros/pdf/g41-llb.pdf>
⁷I. Vincze, *Nucl. Instrum. Methods Phys. Res.* **199**, 247 (1982).
⁸R. N. Corby and P. J. Black, *Acta Crystallogr.* **B29**, 2669 (1973).
⁹M. B. Stearns, *Phys. Rev.* **147**, 439 (1966); I. Vincze and I. A. Campbell, *J. Phys. F: Met. Phys.* **3**, 647 (1973).
¹⁰B. Fultz and Z. Q. Gao, *Nucl. Instrum. Methods Phys. Res. B* **B76**, 115 (1993).
¹¹F. van der Woude and I. Vincze, *J. Phys. (France)* **41**, C1-151 (1980).
¹²V. Niculescu and J. I. Budnick, *Solid State Commun.* **26**, 607 (1978).
¹³A. Geresdi and G. Mihály (private communication).